Interaction of Sulfonated Ruthenium(II) Polypyridine Complexes with Surfactants Probed by Luminescence Spectroscopy

by **David García-Fresnadillo** and **Guillermo Orellana***

Dept. de Química Orgánica, Facultad de Ciencias Químicas, Universidad Complutense de Madrid, E-28040 Madrid

Dedicated to Professor *André M. Braun* on the occasion of his 60th birthday

Novel anionic $[RuL_2L']^{2-}$ complexes, where L stands for (1,10-phenanthroline-4,7-diyl)bis(benzenesulfonate) (pbbs; **3a**) or (2,2′-bipyridine)-4,4′-disulfonate (bpds; **3b**), and L′ is *N*-(1,10-phenanthrolin-5-yl)tetradecanamide (pta; **2a**) or *N*-(1,10-phenanthrolin-5-yl)acetamide (paa; **2b**), were synthesized, and their interaction with the prototypical surfactants sodium dodecylsulfate (SDS), cetyl trimethyl ammonium bromide (CTAB), and *Triton X-100* (TX-100) was investigated by electronic absorption, luminescence spectroscopy, emission-lifetime determinations, and O_2-quenching measurements. $[Ru(pbbs)_2(pta)]^{2-}$ (**5a**) displayed cooperative self-aggregation in aqueous medium at concentrations above 1.3 μM; the observed association was enhanced in the presence of either β-cyclodextrin or NaCl. This amphiphilic Ru^{II} compound showed the strongest interaction with all the detergents tested: nucleation of surfactant molecules around the luminescent probe was observed below their respective critical micellar concentrations. As much as a 12-fold increase of the emission intensity and a 3-fold rise in the lifetime were measured for **5a** bound to TX-100 micelles; the other complexes showed smaller variations. The O_2-quenching rate constants decreased up to 1/8 of their original value in H_2O (*e.g.*, for $[Ru(bpds)_2(pta)]^{2-}$ (**6a**) bound to CTAB micelles). Luminescence-lifetime experiments in H_2O/D_2O allowed the determination of the metal-complex fraction exposed to solvent after binding to surfactant micelles. For instance, such exposure was as low as 25% for pta complexes·CTAB aggregates. The different behaviors observed were rationalized in terms of the Ru^{II} complex structure, the electrostatic/hydrophobic interactions, and the probe environment.

Introduction. – The use of luminophores as 'reporter' probes for sensing (bio)chemical species and microenvironments has been widely documented because of their high sensitivity and specificity [1]. Luminescent Ru^{II} complexes are outstanding molecules in this regard, due to the tuneable photophysical properties of their metal-to-ligand charge-transfer (MLCT) excited state. (Polypyridine)ruthenium(II) complexes display strong absorption bands in the UV/VIS region, orange-red emission at room temperature with a large *Stokes*' shift (*ca.* 200 nm), moderate to good emission quantum yields (0.01 – 0.30), and long luminescence lifetimes (0.1 – 10 μs). In addition, they are thermally and (photo)chemically stable. To tailor applications, the structure of bis- and tris(chelate) complexes of Ru^{II} can be designed by judiciously selecting the nature of the polyazaheterocyclic ligands incorporated in the coordination compound, allowing in this way the possibility of obtaining a whole range of photophysical features for these complexes [2]. This feature makes homoleptic and heteroleptic Ru^{II} complexes very attractive versatile molecules for the development of optical probes and sensors since their photophysical parameters are strongly dependent on the microenvironment around the complex [3]. Not surprisingly, the photophysics of luminescent Ru^{II} complexes in microheterogeneous phases such as those provided by organized media (micelles, bilayers, colloids), biopolymers (DNA and proteins), and

organic/inorganic polymers (poly(vinylsulfate), poly(styrenesulfonate), dendrimers, silica gel, glass, zeolites, *etc.*) has been an area of active research [4].

The interaction of a metal complex with these entities usually produces dynamic binding with the luminophore displaying different spectroscopic properties depending on its location. The distribution of luminescent probes in these microheterogeneous environments is markedly influenced by the hydrophobic/hydrophilic character of the surrounding medium and by the presence of electrostatically charged interfaces. Moreover, restricted spaces with reduced (1–2) or even fractal dimensionalities have to be considered to account for dynamic quenching processes involving the probe molecule [5]. Some of the photophysical and photochemical characteristics of the probe that can be monitored are: absorption and emission spectral shifts, luminescence intensities and lifetimes, emission anisotropy, dynamic or static quenching reactions, sensitization or energy transfer to a second luminophore. Many of these parameters can be strongly affected by the equilibrium constants of the aggregate, the distribution of probe molecules, and the in/out rate constants of the luminophore and other solutes within the timescale of the excited-state deactivation.

Ru^{II} Complexes usually show a strong interaction with anionic, cationic, and neutral surfactants, due to a combination of hydrophobic and electrostatic interactions [6]. Therefore, their luminescence quantum yields and lifetimes generally increase in the presence of the structured microenvironment provided by the surfactants. This is due to protection of the luminophore from quenchers, as well as the increased microviscosity that slows down collisional deactivation of the excited species by restricting their diffusive motions (*e.g.*, quenching by oxygen). On the other hand, their emission maxima remain constant or are slightly shifted depending on the type of complex [4c][6b,c][7]. For instance, multi-exponential emission decays have been observed for $[Ru(bpy)_3]^{2+}$ (bpy = 2,2′-bipyridine) in the presence of surfactants for which the complex displays strong affinity, such as sodium dodecyl sulfate, even at concentrations below its critical micelle concentration (*cmc*) [8].

In spite of the large number of studies on cationic metal complexes carried out by *Demas*, *DeGraff*, and co-workers [6][7] and other authors, there is little information about the behavior of *anionic* Ru^{II} complexes in the presence of surfactants. Our research has aimed the synthesis of novel heteroleptic Ru^{II} complexes with amphiphilic structures, as well as the study of their photophysics in the presence of anionic, cationic, and neutral surfactants, compared to their behavior in homogeneous solution, to evaluate their suitability as optical probes for detergents. In this regard, desired characteristics for maximum sensitivity of the new luminophores are *i*) a strong binding to surfactants *via* hydrophobic/electrostatic interactions, leading to aggregation of the detergent around the luminescent complex; *ii*) an emission quantum yield and lifetime enhancement in the presence of surfactant molecules. To fulfill these requirements, we designed and prepared Ru^{II} complexes containing two polyazaheterocyclic ligands that provide a polar anionic head around the cationic metal center, and a third chelating ligand bearing a long alkyl chain to confer hydrophobicity to the metal complex. For reference purposes, similar Ru^{II} species lacking the long alkyl chain were prepared too. In the structures of these novel $[RuL_2L']^{2-}$ complexes **5** and **6**, L is (1,10-phenanthroline-4,7-diyl)bis(benzenesulfonate) (pbbs; **3a**) or (2,2′-bipyridine)-4,4′-disulfonate

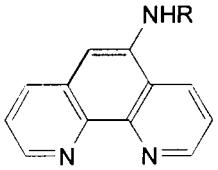

1 R = H
2a R = $Me(CH_2)_{12}CO$, pta
b R = MeCO, paa

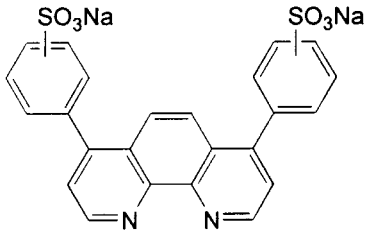

3a · 2 Na, pbbs · $2\ Na^+$

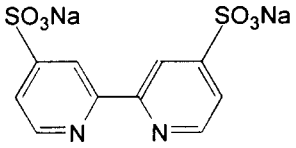

3b · 2 Na, bpds · $2\ Na^+$

$[RuL_2Cl_2]^{4-}$	**4a**	L = pbbs
	b	L = bpds
$[RuL_2L']^{2-}$	**5a**	L = pbbs, L' = pta
	b	L = pbbs, L' = paa
	6a	L = bpds, L' = pta
	b	L = bpds, L' = paa
$[RuL_3]^{4-}$	**7**	L = pbbs
$[RuL_3]^{2+}$	**8**	L = bpy[a])

[a]) bpy = 2,2'-bipyridine (*i.e.*, **3b** without sulfo groups)

(bpds; **3b**), and L′ is *N*-(1,10-phenanthrolin-5-yl)tetradecanamide (pta; **2a**) or *N*-(1,10-phenanthrolin-5-yl)acetamide (paa; **2b**).

The spectroscopy and photophysics of these metal species were studied in aqueous solution and in the presence of prototype anionic (sodium dodecyl sulfate = SDS), cationic (cetyltrimethylammonium bromide = CTAB), and neutral (*Triton X-100* = TX100) surfactants. The degree of exposition to H_2O of the different heteroleptic complexes bound to the corresponding micellar aggregates was also determined, to reveal the nature and strength of the interaction between the Ru^{II} complex and the surfactant, as well as the location of the luminophore bound to the micelle. The tendency to self-aggregation expected for some of the new probes was tested in the presence of additives such as β-cyclodextrin and NaCl [9]. Finally, dissolved O_2-quenching of the luminophores in the absence and in the presence of surfactant micelles was used to confirm the location of the probe in the supramolecular entity.

Results and Discussion. – *Synthesis.* The 1,10-phenanthrolin-5-amine (**1**) was prepared in good yield from 5-nitro-1,10-phenanthroline *via* catalytic reduction with hydrazine hydrate over Pd/C [10]. Attempts to obtain amine **1** *via* reduction with $SnCl_2$ or $Na_2S_2O_4$ provided poor reaction yields. The amide ligands **2a** and **2b** were synthesized from amine **1** following reported methods for the preparation of amides *via* activated carboxylic acids [11], such as the mixed anhydride obtained from tetradecanoic acid and ethyl carbonochloridate, or acetic anhydride. Reaction yields were lower than 50%, due to the low nucleophilic properties of the heteroaromatic amine **1**.

The *N,N′*-dioxide of the disodium salt of the (2,2′-bipyridine)-4,4′-disulfonate was prepared from 2,2′-bipyridine [12]. Reduction of the *N,N′*-dioxide to **3b** was improved by using milder conditions (ammonium formate over 10% Pd/C) than those described by *Balicki* [13].

The *cis*-dichlorobis(chelate)ruthenium(II) complexes **4a** and **4b** were synthesized according to the general method reported by *Sullivan et al.* [14], *i.e.*, by refluxing $RuCl_3$ with a stoichiometric amount of ligand and a high excess of LiCl under inert atmosphere. The high concentration of Cl^- anions in the reaction mixture largely prevented incorporation of a third chelating ligand in the Ru^{II} coordination sphere. The reaction time depended on the structure of the chelating ligand: It was only 5 h for pbbs (**3a**), but 24 h for the bpds (**3b**), due to free rotation between the pyridine rings of **3b** that slowed down chelation. The bis-chelate complexes **4** were isolated together with some amount of LiCl due to the low solubility of this salt in acetone.

There are several methods to prepare tris(chelate)ruthenium(II) complexes with polyazaheterocyclic ligands [15]. Typical reaction conditions for obtaining homoleptic complexes such as **7** and **8** involve heating of $RuCl_3$ and an excess of ligand in a protic solvent (alcohols or mixtures with H_2O) under inert atmosphere. Complexation takes place *via* stepwise incorporation of ligands accompanied by reduction of the metal center by the warm solvent. The synthesis of the heteroleptic complexes **5** and **6** requires previous preparation of the *cis*-dichlorobis(chelate) complexes **4** (see above) and further reaction with excess of the third ligand under similar conditions to those used for the homoleptic complexes.

Photophysical and Electrochemical Characterization. UV/VIS Absorption spectra of the novel heteroleptic complexes **5** and **6** are summarized in *Table 1*, together with those of the homoleptic $[Ru(pbbs)_3]^{4-}$ (**7**) and $[Ru(bpy)_3]^{2+}$ (bpy = 2,2′-bipyridine; **8**) for the sake of comparison. All these species display strong absorption in the VIS region, corresponding to non-degenerated $d \rightarrow \pi^*$ transitions due to symmetry considerations in both the heteroleptic and homoleptic Ru^{II} complexes [16]. The strong UV bands at 215–300 nm arise from intraligand $\pi \rightarrow \pi^*$ transitions. All the investigated complexes display absorption shoulders at *ca.* 315 (**5**) or 350 nm (**6**), due to metal-centered transitions. Complexes **6** show an additional band at *ca.* 265 nm that can be attributed to a more energetic MLCT transition by comparison to the $[Ru(bpy)_3]^{2+}$ (**8**) chromophore [2b]. The absorption maxima of complexes **6** are slightly red-shifted compared to those of **5** and also of **8**, due to the strong electron-withdrawing effect of

Table 1. *Absorption Maxima of the Ru^{II} Complexes in H_2O*

	λ_{abs}^{max} [nm] [a]) (ε [$M^{-1}cm^{-1}$])[b])
5a	460[c]) (36600)[d]), 427[c]) (35650)[d]), 315 (sh, 40200), 274 (175800)[d])
b	459 (22700), 435 (22550), 315 (sh, 21800), 275 (102000), 215 (98600)
6a	466 (17500), 434 (15600), 350 (sh, 12800), 296 (67000), 266 (42300), 218 (72000)
b	466 (16800), 446 (16100), 350 (sh, 12700), 296 (64600), 264 (44800), 218 (71700)
7	462 (29300), 438 (29100), 310 (sh, 35800) 278 (121300), 216 (116400)
8[e])	452 (13700), 344 (sh, 9900), 285 (78100), 243 (24900)

[a]) Experimental error ±1 nm. [b]) Experimental error ±3%. [c]) Experimental error ±3 nm. [d]) Experimental error ±8%. [e]) [24].

the SO_3^- substituents that increases the π-acceptor character of the bpds ligand and, consequently, lower the energy of their π^* orbitals. This effect is less important in the pbbs ligand, the SO_3^- groups of which are placed at the distal end of a more extended aromatic structure. The absorption coefficients of **6** are lower than those of **5** and $[Ru(pbbs)_3]^{4-}$ (**7**) due to the smaller absorption cross-section of the sulfonated ligands included in the former complexes.

All the investigated Ru^{II} complexes display a broad emission band in the VIS region of the electromagnetic spectrum at room temperature. Luminescence maxima in different solvents are collected in *Table 2*. The actual position of the emission band depends on the solvent. This result was to be expected since the electronically excited Ru^{II} complexes are very sensitive to their environment [2]. As it is observed in the absorption spectra, the luminescence of bpds complexes appears at longer wavelengths than that of the corresponding pbbs complexes. Similar reasons to those outlined above may account for such differences. The only exceptions are the spectra recorded in DMF solvent, where all the Ru^{II} complexes display the same emission maximum (*Table 2*).

Table 2. *Emission Maxima of the Ru^{II} Complexes in H_2O and Organic Solvents*

	λ_{em}^{max} [nm][a])				
	H_2O	MeOH	EtOH	DMF	MeCN/H_2O 1:1
5a	624	620	616	636	624
b	629	622	623	636	631
6a	650	645	637	638	649
b	652	645	640	638	648
7	632	618	–[b])	637	–[b])
8	630[c])	620[d])	608[d])	635	620[d])

[a]) Corrected for the instrumental response; estimated error ±3 nm. [b]) Not determined, due to the very low solubility of the Ru^{II} complex. [c]) [34]. [d]) [35]. [e]) In MeCN [36].

The different nature of the pbbs and bpds ligands strongly influences the emission quantum yield and lifetime of the corresponding complexes **5** and **6** in H_2O. *Table 3* collects the luminescence quantum yields Φ_{em}, the emission lifetimes under Ar (τ_0) and air-equilibrated (τ), the unimolecular deactivation rate constants k_r (radiative) and k_{nr} (non-radiative), and the fraction $F_{O_2}^T$ of ^{3}MLCT excited states quenched by oxygen, for all the studied complexes in H_2O. Those with the pbbs ligand have Φ_{em} values larger than 0.15 and τ_0 values around 3.8 μs. However, the Ru^{II} complexes containing bpds have *ca.* 7-fold smaller luminescence quantum yields and lifetimes. The presence of polypyridine ligands with Ph substituents at positions 4 and 7 significantly increases Φ_{em} and τ_0 of the corresponding Ru^{II} complexes, as it has been reported for Ru^{II} coordination compounds with substituted 2,2′-bipyridine and 1,10-phenanthroline ligands [17]. This result can be explained by the larger k_{nr} values of the luminpophores **6** (*Table 3*). The quenching rate constants by oxygen of the investigated Ru^{II} complexes are in the range $1-4\cdot10^9$ $M^{-1}s^{-1}$ (see below), a value close to the diffusion limit of the

kinetics in aqueous solution [18]. Nevertheless, k_q constants are slightly lower for the bpds complexes **6**. The longer emission lifetime of the pbbs complexes **5** and **7** compared to that of the bpds chelates **6** (*Table 3*), together with the corresponding quenching rate constants, may account for the significantly higher oxygen-quenching probability of the pbbs ($F^T_{O_2} \approx 0.75$) *vs.* the bpds complexes ($F^T_{O_2} \approx 0.15$).

Table 3. *Photophysical Parameters and Probability of Excited-State Quenching by Oxygen of the Ru^{II} Complexes in Water* [a])

	Φ_{em} [b])	τ_0 [μs] [b])	τ [μs] [c])	k_r [$10^4 s^{-1}$] [b])	k_{nr} [$10^5 s^{-1}$] [b])	$F^T_{O_2}$ [c]),[d])
5a	0.17	3.70	1.05[e])	4.6	2.2	0.72
b	0.20	3.83	0.99	5.1	2.0	0.74
6a	0.031	0.48	0.39	6.4	20	0.19
b	0.024	0.40	0.36	6.0	24	0.10
7	0.15	3.80	0.90	3.9	2.2	0.76
8	0.042[f])	0.61[g])	0.39	6.9	16	0.36

[a]) [Ru^{II}] ≤ 10 μM except otherwise stated. [b]) Ar-Purged solutions; estimated error ±5% (Φ_{em}), ±2% (τ_0), ± 10% (k_r and k_{nr}). [c]) Air-equilibrated solutions; estimated error ±2% (τ), ±10% (k_q), ±10% ($F^T_{O_2}$). [d]) Fraction of luminophore ^{3}MLCT excited states quenched by oxygen. [e]) At 1.0 μM concentration; estimated error ±5%. [f]) [19a]. [g]) [24].

The emission lifetimes of the novel luminophores in organic solvents are given in *Table 4*. The pbbs complexes **5** display a longer emission lifetime in H_2O than in organic solvents. However, the photoexcited bpds complexes **6** live longer in organic solvents. This behavior can be rationalized in terms of excited-state quenching due to reaction with dissolved oxygen and/or due to the non-radiative deactivation pathway by energy transfer by the solvent OH oscillators in the different media [2b][19]. The solubility of O_2 in air-equilibrated organic solvents is *ca.* 10 times higher than in air-equilibrated H_2O [20]. Those complexes that are efficiently quenched by oxygen (large $F^T_{O_2}$, *Table 3*), such as **5a** and **5b**, will show shorter luminescence lifetimes in organic media. However, since oxygen quenching of complexes **6** is poor (small $F^T_{O_2}$), the excited-state lifetime is controlled by the fast non-radiative deactivation (*Table 3*). In this way, the less efficient energy transfer to the organic solvent OH oscillators compared to H_2O yields longer emission lifetimes in the former media (*Table 4*).

Table 4. *Emission Lifetimes of the Novel Ru^{II} Complexes in Air-Equilibrated Organic Solvents* [a])

	τ [μs] [b])		
	MeOH	EtOH	MeCN/H_2O 1:1
5a	0.30	0.38	0.43
b	0.32	0.39	0.47
6a	0.45	0.60	0.50
b	0.44	0.54	0.49

[a]) [Ru^{II}] ≤ 10 μM. [b]) Experimental error ±2%.

With the exception of $[Ru(pbbs)_2(pta)]^{2-}$ (**5a**), the luminescence decay kinetics of the new Ru^{II} complexes in H_2O is strictly exponential. The former shows a single-exponential decay profile at 1 μM concentration, but a bi-exponential fit is required in more concentrated aqueous solutions. These results point out *spontaneous self-aggregation* of the pbbs/pta coordination compound **5a**. The structure of this species may be described as an amphiphilic molecule having a bulky anionic head and a long (hydrophobic) aliphatic tail. To investigate this phenomena and its possible occurrence in the other new Ru^{II} complexes, especially those involving the pta ligand, their absorption and emission features were investigated in the 1–100 μM concentration range (data not shown). These experiments established that all the complexes follow the *Lambert-Beer* law in the concentration range studied, except $[Ru(pbbs)_2(pta)]^{2-}$ (**5a**), for which the absorbance *vs.* concentration plot is linear just up to 50 μM. In every case, the emission intensity increases linearly with the luminophore concentration in the 1–10 μM interval. Higher concentrations lead to classical inner-filter effects. Only for Ru^{II} complex **5a**, the emission decay kinetics display different profiles depending on its concentration in H_2O: at higher values than 3 μM, bi-exponential functions have to be used to fit the emission decay curves (*Table 5*). To compare the luminescence lifetimes of the probes in different media and at various concentrations, the so-called pre-exponential weighted mean lifetime, τ_M (*Table 5*) was calculated according to $\tau_M = \Sigma(\alpha_i\tau_i)/\Sigma\alpha_i$ [21], where α_i are the normalized pre-exponential factors and τ_i the reciprocal of the time constants for each component of the multi-exponential fit. The data of *Table 5* show that τ_M increases almost two-fold with the concentration of $[Ru(pbbs)_2(pta)]^{2-}$ (**5a**) in H_2O. Its luminescence lifetime levels off at 50 μM complex. This behavior may be explained if different emitting species co-exist in solution. The short-lived species display decay kinetics similar to that observed in 1 μM solutions (*ca.* 1.0 μs lifetime) and can be attributed to isolated molecules of the Ru^{II} complex. The long-lived species (*ca.* 2.8 μs) would correspond to aggregates of $[Ru(pbbs)_2(pta)]^{2-}$ (**5a**) molecules, whose contribution to the overall emission increases with concentration. The longer luminescence lifetime of the aggregates would be due to a higher protection of the excited state from oxygen quenching and deactivation by the solvent. As can be seen in *Fig. 1*, since the τ_M value reaches a plateau above 50 μM complex, the aggregates seem to have a defined size. This behavior by which individual molecules in

Table 5. *Bi-exponential and Pre-exponential Weighted Emission Lifetimes τ_M of $[Ru(pbbs)_2(pta)]^{2-}$* (**5a**) [a][b])

Concentration [μM]	τ_1 [μs]	(%)[c])	τ_2 [μs]	(%)[c])	τ_M [μs]
1.0	1.05	100	–	–	1.1
3.0	0.91	91	2.3	9	1.0
7.0	1.02	88	2.7	12	1.2
10	1.07	72	2.3	28	1.4
25	1.04	68	2.6	32	1.5
50	0.91	54	2.9	46	1.8
75	0.94	54	2.7	46	1.8
100	0.93	54	2.8	46	1.8

[a]) Air-equilibrated aqueous solution. [b]) Estimated error in τ and $\tau_M \pm 10\%$. [c]) Contribution to the overall decay calculated as $\tau_i\ \% = (\alpha_i/\Sigma\alpha_i) \cdot 100$.

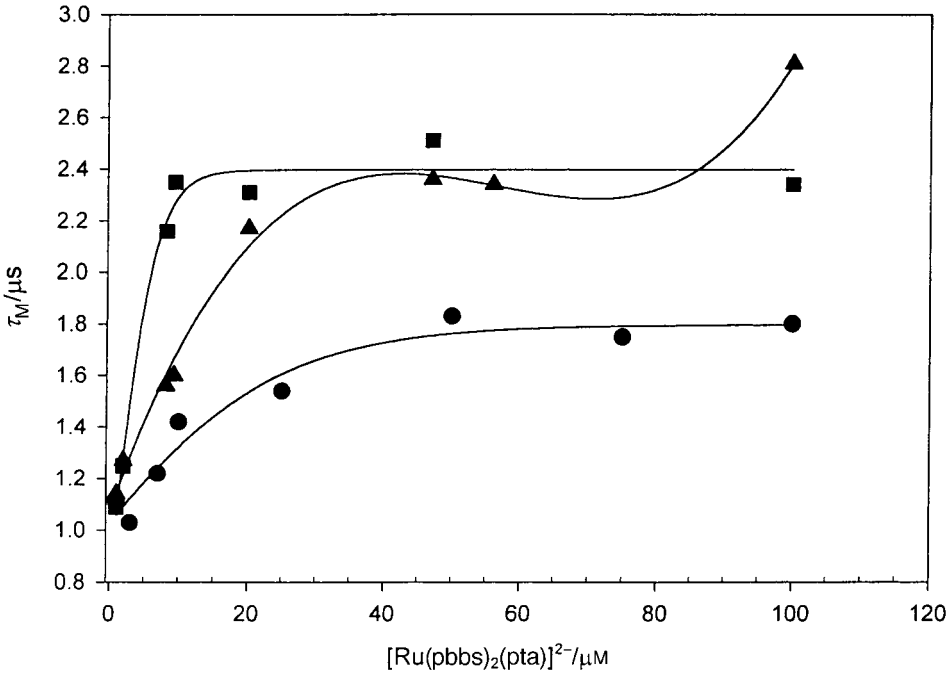

Fig. 1. *Emission lifetime of [Ru(pbbs)$_2$(pta)]$^{2-}$* (**5a**) *at different concentrations in water* (●) *and in the presence of 10 μM β-cyclodextrin* (▲) *or 10 mM NaCl* (■)

equilibrium with aggregates are present in solution is that of classical amphiphilic molecules [1].

To elucidate the importance of hydrophobic and electrostatic interactions in self-aggregation of the novel Ru^{II} complexes, their luminescence lifetimes were measured in the presence of β-cyclodextrin or NaCl. Metal complexes **5b**, **6a**, and **6b** displayed again no sign of association in the investigated additive concentration range (5–200 μM β-cyclodextrin, 0.01–1.0M NaCl), since their excited-state lifetimes remained unchanged. The possible reason for the lack of self-aggregation of $[Ru(bpds)_2(pta)]^{2-}$ (**6a**) despite its amphiphilic character could be the size and high negative charge of its polar head, making much more important the electrostatic repulsion than the stabilizing hydrophobic interactions occurring in micelles. Unlike its bpds analogue, the emission lifetime of $[Ru(pbbs)_2(pta)]^{2-}$ (**5a**) is strongly increased upon addition of either β-cyclodextrin (10 μM) or NaCl (10 mM) (see *Fig. 1*). A plateau at $\tau_M \approx 2.4$ μs is reached in the presence of those additives, pointing out that their ^{3}MLCT excited state is more efficiently protected from dissolved oxygen and/or solvent deactivation. The luminescence lifetime of **5a** in pure H_2O levels off at 50 μM concentration. In the presence of β-cyclodextrin or NaCl, the concentration of **5a** at which a plateau in τ_M is reached decreases to *ca.* 30 and 10 μM, respectively. This behavior can be interpreted in terms of a higher tendency to self-association, together with a change of the aggregate structure, since τ_M of the complex at the plateau is longer. NaCl is more efficient than β-cyclodextrin in inducing self-association: a higher ionic strength decreases the

electrostatic repulsion between the anionic heads allowing the formation of more compact aggregates. Insertion of the pbbs ligand into the hydrophobic cavity of β-cyclodextrin would also decrease the electrostatic repulsion between the polar heads of $[Ru(pbbs)_2(pta)]^{2-}$ (**5a**) to produce more compact aggregates, too.

Since self-association of $[Ru(pbbs)_2(pta)]^{2-}$ (**5a**) in H_2O occurs at μM concentrations (*Table 5* and *Fig. 1*), the onset of the aggregation process was determined by measuring the changes in the surface tension of H_2O upon addition of the Ru^{II} complex **5a** (*Fig. 2*). Corroborating the conclusions from emission lifetime data, aggregation of the luminophore was found to occur at 1.35 ± 0.07 μM. The high tendency to self-binding of this metal complex results from its long alkyl chain and bulky polar head, which has also some hydrophobic character that favors lipophilic interactions that are little disturbed by electrostatic repulsions.

Redox Potentials. The electrochemical features of the ground and excited states of the novel Ru^{II} complexes and the prototypes $[Ru(pbbs)_3]^{4-}$ (**7**) and $[Ru(bpy)_3)]^{2+}$ (**8**) are collected in *Table 6*. Cyclic-voltammetry experiments show one oxidation and three reduction waves in DMF at room temperature. These waves correspond to the quasi-reversible monoelectronic redox processes typical for Ru^{II} complexes, since the sulfonate and amide substituents are electrochemically stable [2b][22]. The redox potentials of the anionic complexes in their ground state agree well with those observed for the related homoleptic complexes $[Ru(pbbs)_3]^{4-}$ (**7**) and $[Ru(bpy)_3]^{2+}$ (**8**) in DMF (*Table 6*). The corresponding redox potentials of the ^{3}MLCT excited state were obtained according to the method of *Lin et al.* and are very close to those calculated for

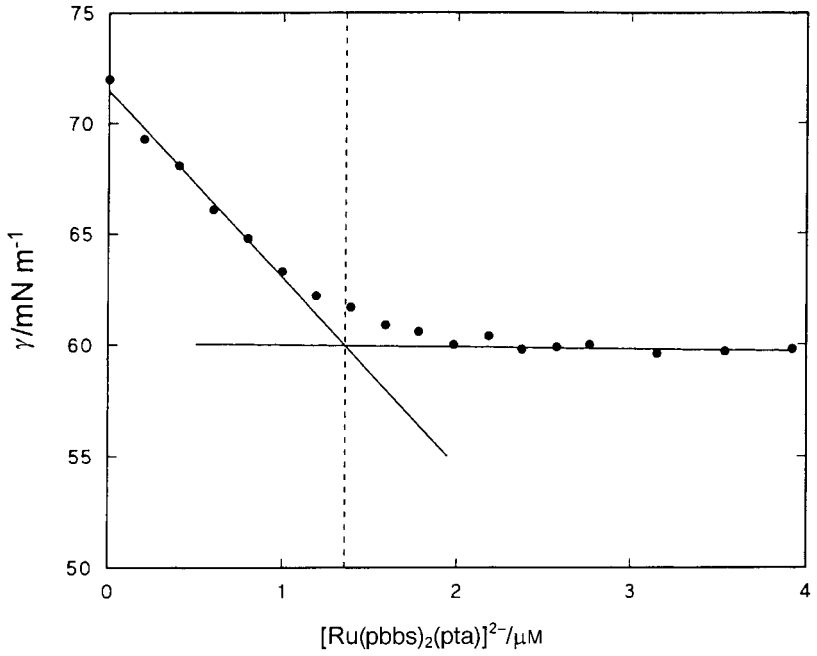

Fig. 2. *Variation of the surface tension γ of $[Ru(pbbs)_2(pta)]^{2-}$ (**5a**) aqueous solutions as a function of the metal-complex concentration*

Table 6. *Redox Potentials* (in V *vs.* SCE) *of the Ground and Excited States of the Ru^{II} Complexes in DMF at 23 ± 2°*

	Oxidation[a])		Reduction[a])				
	$E^0_{(3+/2+)}$	$E^0_{(3+/2+*)}$[b])	$E^0_{(2+/+)}$	$E^0_{(2+*/+)}$[c])	$E^0_{(+/0)}$	$E^0_{(0/-)}$	$E_{0\text{-}0}$ [eV][d])
5a	1.27	– 0.83	– 1.25	0.85	– 1.37	– 1.57	2.10
b	1.24	– 0.86	– 1.24	0.86	– 1.40	– 1.65	2.10
6a	1.29	– 0.80	– 1.23	0.86	– 1.40	– 1.68	2.09
b	1.29	– 0.80	– 1.24	0.85	– 1.43	– 1.69	2.09
7	1.25	– 0.84	– 1.24	0.85	– 1.35	– 1.56	2.09
8	1.29	– 0.81	– 1.25	0.85	– 1.42	– 1.69	2.10

[a]) Estimated error ± 0.03 V. [b]) $E^0_{(3+/2+*)} = E^0_{(3+/2+)} - E_{(0\text{-}0)}$. [c]) $E^0_{(2+*/+)} = E^0_{(2+/+)} + E_{(0\text{-}0)}$. [d]) Energy of the 0-0 transition from the ^{3}MLCT excited state to the ground state.

the $*[Ru(bpy)_3]^{2+}$ complex [23]. The similarity, within experimental error, between the ground- and excited-state oxidation/reduction potentials observed for all the complexes is in agreement with the observed uniformity of their luminescence maxima in DMF (636–638 nm), demonstrating once again the coincidence between the redox and spectroscopic orbitals of those species [24].

Luminescence Measurements in Surfactant Solution. The number of probes in the micelle should not be large since too many interacting species disturb the micellar structure [1d]. Therefore, we chose an occupation-number [1a] close to one Ru^{II} complex per micelle. All the experiments were performed at surfactant concentrations in the order of their respective critical micelle concentration (*cmc*) to follow the changes in the photophysical properties of the investigated luminophore during the micellization process. Therefore, the experiments with SDS (*cmc* = 8.0 mM, aggregation number 62) [1d] were carried out at 1 μM probe, for a 0–12 mM surfactant-concentration range. Measurements with CTAB (*cmc* = 0.92 mM, aggregation number 60) [1d] were performed at 0.3 μM probe, for a 0–15 mM detergent-concentration range. The experiments with TX-100 (*cmc* = 0.24 mM, aggregation number 140) [1d] were carried out at 0.5 μM probe, for a 0–0.35 mM surfactant concentration range. The variations in the luminescence intensities and lifetimes of the anionic Ru^{II} complexes in the presence of detergents are depicted in *Figs. 3–5*.

Measurements in the Presence of SDS. No changes in the wavelength of the MLCT absorption maxima of the $[RuL_2L']^{2-}$ complexes are detected upon addition of SDS. However, in the presence of an increasing concentration of the anionic surfactant, $[Ru(pbbs)_2(pta)]^{2-}$ (**5a**) displays a strong hyperchromic shift in its absorption spectrum. At 4 mM SDS, the absorbance is twice as much as that of the complex in the absence of detergent, and it keeps constant at higher surfactant concentrations. This behavior can be attributed to light scattering due to pre-micellization of the surfactant around the luminophore. The induced formation of micelles in the presence of an added solute at surfactant concentrations below its 'normal' *cmc* was firstly suggested to explain the spectral changes of pinacyanol in SDS [7c][25]. The variation in the emission intensity of the complexes with the SDS concentration is shown in *Fig. 3*, *a*. No shifts in the position of the luminescence maximum are detected for **5a**, but it displays a strong signal enhancement in the 0–8 mM SDS range, with a very steep

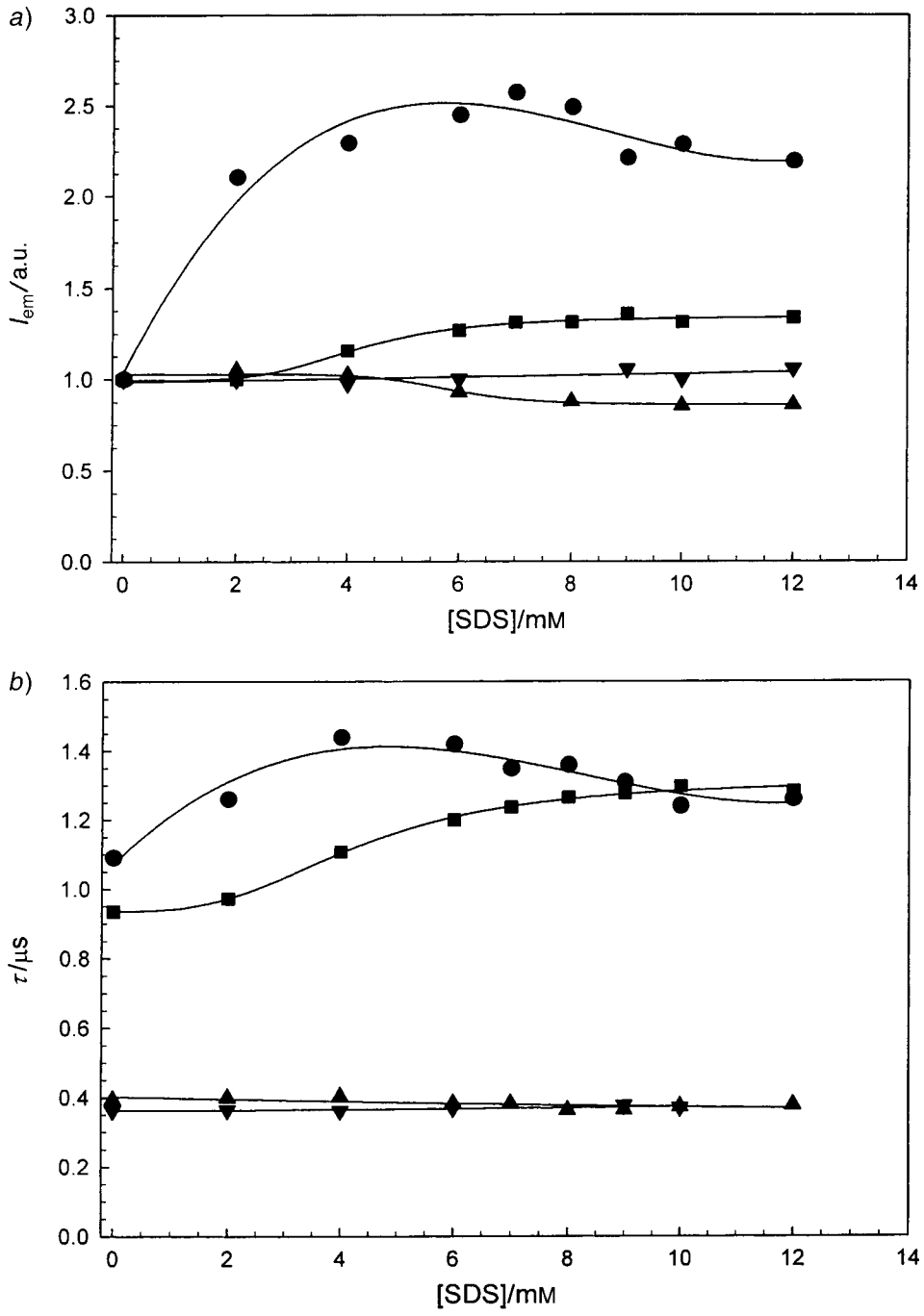

Fig. 3. a) *Normalized emission intensity and* b) *lifetimes of the* $[RuL_2L']^{2-}$ *complexes* (1 μM in air-equilibrated water) *in the presence of SDS:* $[Ru(pbbs)_2(pta)]^{2-}$ (**5a**; ●), $[Ru(pbbs)_2(paa)]^{2-}$ (**5b**; ■), $[Ru(bpds)_2(pta)]^{2-}$ (**6a**; ▲), *and* $[Ru(bpds)_2(paa)]^{2-}$ (**6b**; ▼)

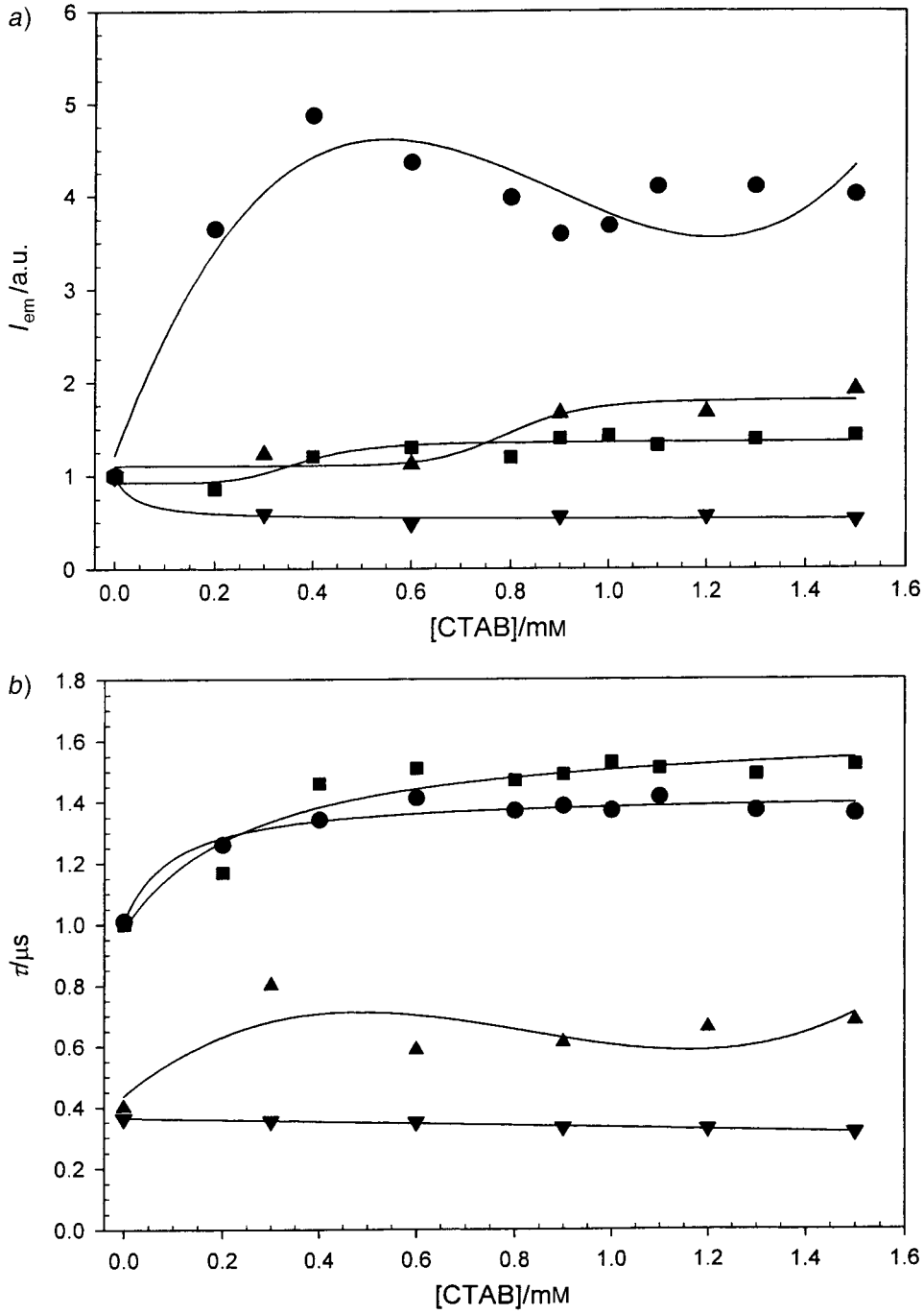

Fig. 4. a) *Normalized emission intensity and* b) *lifetimes of the* $[RuL_2L']^{2-}$ *complexes* (0.3 μM in air-equilibrated water) *in the presence of CTAB:* $[Ru(pbbs)_2(pta)]^{2-}$ (**5a**; ●), $[Ru(pbbs)_2(paa)]^{2-}$ (**5b**; ■), $[Ru(bpds)_2(pta)]^{2-}$ (**6a**; ▲), $[Ru(bpds)_2(paa)]^{2-}$ (**6b**; ▼)

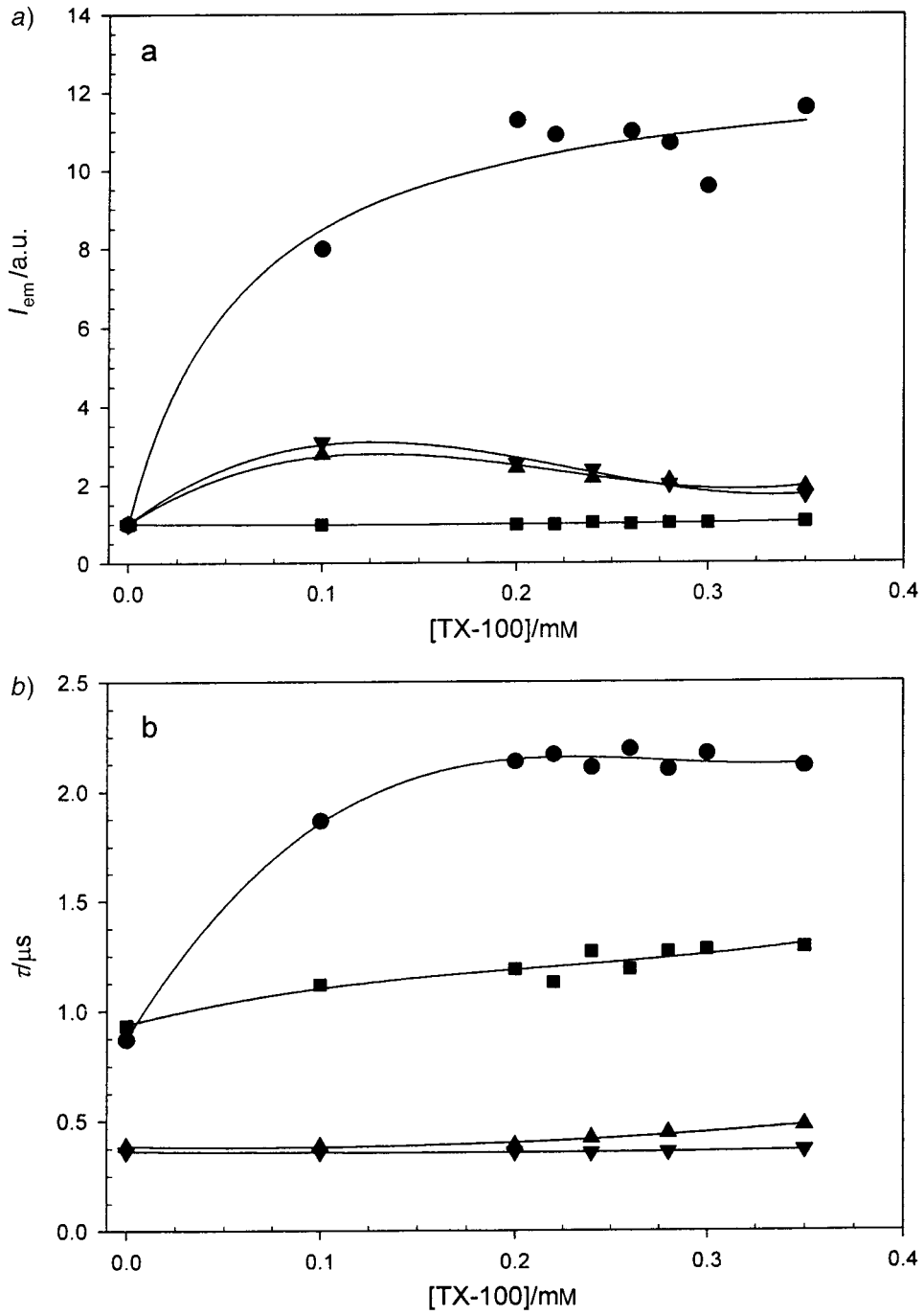

Fig. 5. a) *Normalized emission intensity and* b) *lifetimes of the* $[RuL_2L']^{2-}$ *complexes* (0.5 μM in air-equilibrated water) *in the presence of Triton X-100:* $[Ru(pbbs)_2(pta)]^{2-}$ (**5a**; ●), $[Ru(pbbs)_2(paa)]^{2-}$ (**5b**; ■), $[Ru(bpds)_2(pta)]^{2-}$ (**6a**; ▲), *and* $[Ru(bpds)_2(paa)]^{2-}$ (**6b**; ▼)

increment in the 0–2 mM SDS range, in agreement to the proposed pre-micellization of the detergent around the Ru^{II} complex [6b]. The maximum luminescence intensity is reached around 7 mM SDS, a value close to the detergent *cmc* (8.0 mM) [1d]. For SDS concentrations above these value, a plateau in the emission intensity is reached. The emission lifetimes of the complexes in the presence of SDS are depicted in *Fig. 3*, *b*. All the probe molecules display strictly exponential emission kinetics. The results for **5a** parallel those obtained with the steady-state measurements. There seems to be preconcentration of surfactant molecules around the luminophore at SDS concentrations below its *cmc*, shown by an increase of τ, and a plateau value (1.3 μs) is reached thereafter. These changes are due to some protection of the ^{3}MLCT excited state of the complex by the interacting surfactant molecules. The luminescence intensity and lifetime measured at SDS concentration above its *cmc* can be the consequence of stabilization of the structure of the luminophore·surfactant aggregates, since the experimental conditions were adjusted to maximize the number of singly-occupied micelle (see above). The fractional exposure to H_2O (*f* value; see *Exper. Part*) of $[Ru(pbbs)_2(pta)]^{2-}$ in the presence of SDS micelles was calculated from the emission lifetime data in H_2O and D_2O (*Table 7*). The resulting *f* value, 0.72 (*Table 8*), demonstrates a rather weak interaction with the detergent micelles since it would mean that, on the average, *ca.* 2/3 of complex **5a** are exposed to the solvent molecules. This might be due to the large size of the Ru^{II} complex and to the absence of favorable

Table 7. *Luminescence Lifetimes (τ_0/μs) of the Novel Ru^{II} Complexes in H_2O and D_2O Solution in the Presence of SDS, CTAB, or TX-100 Micelles* [a])

	τ_0/μs							
	No detergent		SDS[b])		CTAB[c])		TX-100[d])	
	H_2O	D_2O	H_2O	D_2O	H_2O	D_2O	H_2O	D_2O
5a	3.7	5.4	4.8	6.8	3.4	3.7	5.6	6.5
b	3.8	5.6	4.8	6.4	5.4	6.2	4.9	6.2
6a	0.48	0.95	0.46	0.92	0.71	1.1	0.56	1.0
b	0.40	0.79	0.41	0.81	0.47	0.82	0.40	0.79

[a]) Ar-purged solutions at 25°; 10 μM complex concentration, except for **5a** ($\leq$ 1.2 μM); estimated error ±2%. [b]) $20 < [SDS] < 33$ mM. [c]) [CTAB] = 13 mM, except for **5a** (1.3 mM). [d]) [TX-100] = 5 mM, except for **5a** ($16 \leq$ [TX-100] $\leq$ 33 mM).

Table 8. *Fractional Exposure to H_2O (f) of the Novel Ru^{II} Complexes in Micellar Aqueous Solutions of SDS, CTAB, and TX-100 at 25°* [a])

	f Value		
	SDS	CTAB	TX-100
5a	0.72 ± 0.06	0.24 ± 0.03	0.29 ± 0.02
b	0.59 ± 0.05	0.27 ± 0.02	0.52 ± 0.04
6a	1.05 ± 0.05	0.48 ± 0.02	0.77 ± 0.04
b	0.97 ± 0.06	0.72 ± 0.04	1.00 ± 0.06

[a]) Calculated from data of *Table 7* (see also *Exper. Part*).

electrostatic interactions with the micelle, in addition to hydrophobic interactions with the long alkyl chain. This result agrees nicely with the observed quenching rate constant of the luminophore by oxygen: k_q (*Table 9*) decreases slightly in going from aqueous solution to SDS micelles (2.7 *vs.* $2.1 \cdot 10^9$ $M^{-1}s^{-1}$), as expected for a weak protection of the photoexcited probe.

Table 9. *Quenching Rate Constants* ($k_q/10^9$ $M^{-1}s^{-1}$) *of the Novel* Ru^{II} *Complexes by Oxygen in* H_2O *and in Micellar Aqueous Solutions of SDS, CTAB, and TX-100 at 25°*[a])

	$k_q/10^9$ $M^{-1}s^{-1}$			
	H_2O	SDS	CTAB	TX-100
5a	2.7	2.1	1.8	1.2
b	3.0	2.2	1.9	2.3
6a	1.9	1.8	0.25	1.2
b	1.1	1.1	–[b])	0.8

[a]) Experimental error ± 10%. [b]) Not determined.

$[Ru(pbbs)_2(paa)]^{2-}$ (**5b**) displays a similar behavior to that of **5a** as far as its absorption and emission features is concerned, but to a smaller extent (*Fig. 3*). This result indicates that the absence of a long alkyl chain negatively influences the nucleation process of the surfactant around the luminophore molecule. The fractional exposure of **5b** to H_2O in the presence of SDS micelles is calculated to be 0.59 (*Table 8*), indicating some protection of the MLCT excited state in the supramolecular entity, as shown by the emission intensity and lifetime data. This result is corroborated by the 20% decrease of the oxygen-quenching rate constant (*Table 9*), as also observed for complex **5a**.

Ru^{II} Complexes **6a** and **6b** do not exhibit any hyperchromic shift of their absorption spectra and negligible changes in their emission features in the examined SDS concentration range, pointing out the lack of interaction with SDS. This finding is further supported by the unity *f* values measured for **6a** and **6b** (*Table 8*), as well as by identical oxygen-quenching rate constants determined in H_2O and in SDS solution (*Table 9*). Such behavior would be due to an important repulsive effect of the anionic Ru^{II} complex, having a high charge density, and the anionic micelle, which is not balanced by peripheral hydrophobic benzene rings such as those contained in the pbbs ligand.

Measurements in the Presence of CTAB. No changes in the wavelength of the MLCT transition of the $[RuL_2L']^{2-}$ complexes are detected upon addition of CTAB. However, the position of their emission band is not constant, and while exponential luminescence decays are measured for complexes **5b**, **6a**, and **6b**, this is not always the case for $[Ru(pbbs)_2(pta)]^{2-}$ (**5a**). Random variations in the absorbance of the Ru^{II} complexes are observed in the presence of the cationic surfactant. This fact is due to a slow appearance of $[RuL_2L']^{2-}$/CTAB precipitates after ion-pair formation. The variations in the emission intensity of the complexes with the CTAB concentration are displayed in *Fig. 4,a*. Since the Ru^{II} concentrations are lower than in the absorption experiments, no precipitation is observed upon addition of the detergent. The complex $[Ru(pbbs)_2(pta)]^{2-}$ (**5a**) shows a 12-nm red shift in its emission maximum in the

presence of CTAB. The observed bathochromic shift can be ascribed to a somewhat less polar environment experienced by the Ru^{II} complex (see the emission maximum in H_2O compared to a non-protogenic solvent such as DMF, *Table 2*), as it might be expected for a luminescent probe buried in the micelle. This observation is also supported by the dramatic luminescence enhancement that occurs in the 0–0.4 mM CTAB range, indicating efficient pre-micellization of surfactant molecules around the Ru^{II} complex, even at very low detergent concentrations. The maximum intensity is reached at 0.4 mM CTAB, far below its *cmc* value (0.92 mM) [1d]. For CTAB levels above 0.4 mM, a slight decrease occurs, and a plateau is reached. The variations in the emission lifetimes of the probes with the CTAB concentration are shown in *Fig. 4,b*. Single-exponential decays are observed for all the complexes, except for $[Ru(pbbs)_2(pta)]^{2-}$ (**5a**), for which bi-exponential fits are required. This complex displays single-exponential decays at $[CTAB] \geq 1.3$ mM. Therefore, pre-exponential weighed mean lifetimes are used in *Fig. 4,b* for complex **5a** at low CTAB concentrations. Its luminescence lifetime increases as minute amounts of CTAB are added to the solution, and a plateau value (1.4 μs) is reached at only 0.4 mM CTAB. The strong interaction between Ru^{II} complex **5a** and CTAB is confirmed by its low fractional exposure to H_2O in the presence of CTAB micelles ($f = 0.24$, *Table 8*), *i.e.*, only about 1/4 of this luminescent probe is in contact with the aqueous environment. The very efficient protection of the ^{3}MLCT excited state of **5a** by CTAB micelles is also supported by a lower oxygen-quenching rate constant in surfactant medium (*Table 9*).

$[Ru(pbbs)_2(paa)]^{2-}$ (**5b**) also shows an increase in its emission intensity, and lifetime (*Fig. 4*). The absence of a long aliphatic chain in **5b** has an effect on the nucleation of the surfactant molecules around the luminophore, since the pre-micellization process starts at higher CTAB concentrations compared to **5a**. The latter complex also shows a 12-nm red shift of its emission maximum in the presence of CTAB, demonstrating the strong interaction of both complexes with the detergent. The low fraction of solvent exposure observed for **5b** ($f = 0.27$, *Table 8*) agrees with the proposed efficient association with CTAB micelles, largely due to favorable electrostatic interactions. The lower oxygen-quenching rate constant observed (*Table 9*) also supports this result.

The complexes $[Ru(bpds)_2(pta)]^{2-}$ (**6a**) and $[Ru(bpds)_2(paa)]^{2-}$ (**6b**) behave differently. The former displays a slight emission enhancement and longer lifetimes at CTAB concentrations close to its *cmc* due to electrostatic and hydrophobic interactions, but shows a progressive 8-nm blue shift in its luminescence maximum with increasing CTAB concentration. Unlike the pbbs complexes, the hypsochromic shift has also been observed when the bpds chelates are dissolved in DMF compared to their emission maxima in H_2O (*Table 2*). The observed destabilization of the ^{3}MLCT excited state can be attributed to a less polar environment experienced by the charge-dense Ru^{II}(bpds) species, as it would occur for a probe partially protected from the H_2O molecules by the cationic micelle. Complex **6b** does not show any change in the position of its emission band, indicating that it is mainly surrounded by an aqueous environment. A decrease of *ca.* 50% in its emission intensity is observed, even at very low CTAB concentration (*Fig. 4, a*) due to luminescence quenching in the ion pair. This effect is also noticed in the emission lifetime. The different behavior of **6a** and **6b** can be rationalized by the effect of the alkyl chain, *i.e.*, the existence or absence of

hydrophobic interactions. It is likely that, despite the favorable electrostatic attraction between the complexes and the polar heads of the CTAB molecules, the geometry of the aggregates is different in these two cases. Therefore, it is not surprising that the degree of exposure to solvent for **6a** and **6b** is different ($f = 0.48$ and 0.72, resp.). While the pta complex **6a** interacts significantly with the CTAB micelle, its paa analogue **6b** experiences mainly an aqueous environment. The oxygen-deactivation constant of **6a** bound to CTAB micelles is 8-fold lower than its value in H_2O (*Table 9*), due to very effective protection of the luminophore from the quencher approach. The oxygen-quenching rate constant for **6b** could not be determined, due to the luminescence quenching observed in the presence of CTAB (see above).

Measurements in the Presence of TX-100. No changes in the position of the MLCT absorption band of the $[RuL_2L']^{2-}$ complexes are detected upon addition of TX-100. All of them, with the exception of $[Ru(bpds)_2(paa)]^{2-}$ (**6b**), display a hyperchromic shift in their absorption spectrum, due to pre-micellization of the surfactant around the luminophore. The variation of their emission intensity with the TX-100 concentration is depicted in *Fig. 5*, *a*. $[Ru(pbbs)_2(pta)]^{2-}$ (**5a**) shows a very strong luminescence enhancement in the 0–0.2 mM TX-100 range. Its emission intensity levels off at this concentration, near to the TX-100 *cmc* (0.24 mM) [1d]. Moreover, a 4-nm bathochromic shift of the emission band is observed in the presence of the non-ionic surfactant. Such behavior reveals the strong tendency to association between the amphiphilic complex **5a** and TX-100. The effect of this detergent on the emission lifetimes of the Ru^{II} complexes is displayed in *Fig. 5*, *b*. The luminescence decay profiles observed for all the probes fit to single-exponential functions. Once again $[Ru(pbbs)_2(pta)]^{2-}$ (**5a**) shows the largest variation (2.5-fold) in its excited-state lifetime upon addition of TX-100, in agreement with the steady-state results. The value of τ reaches a plateau (2.1 μs) at about TX-100 *cmc*. The calculated fractional exposure of **5a** to H_2O in the presence of TX-100 micelles is 0.29 (*Table 8*), indicating that only one third of the complex lies in the aqueous phase, and pointing out a high protection of its MLCT excited state. The oxygen-quenching rate constant of **5a** bound to TX-100 micelles is about half of the value measured in H_2O (*Table 9*), a result consistent with a deeper location of the probe in the micellar surface.

Unlike **5a**, neither the emission intensity nor the band position of $[Ru(pbbs)_2(paa)]^{2-}$ (**5b**) undergo any change in the presence of TX-100. This complex exhibits a small emission-lifetime increase on addition of the surfactant, due to a weak interaction, as the solvent-exposure fraction (0.52, *Table 8*) points out too. This result is also supported by a k_q value only slightly lower than that measured in H_2O and similar to that observed in the presence of SDS (*Table 9*). All these data indicate that the hydrophobic alkyl chain is a key structural element for an efficient interaction and nucleation of the neutral surfactant around the Ru^{II} complex, since binding of these probes to non-ionic micelles has been reported to be controlled by non-electrostatic interactions [6c].

$[Ru(bpds)_2(pta)]^{2-}$ (**6a**) and $[Ru(bpds)_2(paa)]^{2-}$ (**6b**) show a different behavior compared to the pbbs-containing complexes. Both probes display a 30-nm blue shift in their emission band on the first addition of TX-100 (0.1 mM final concentration). This large hypsochromicity progressively decreases in the presence of more concentrated TX-100 solutions, until a spectral position similar to that of the complexes in H_2O is

recovered at detergent concentrations above its *cmc*. Such a result can be explained if a pre-micellar association takes place, since the weakly polar ethoxyalkyl groups of TX-100 would provide less stabilization to the highly dipolar MLCT excited state than when the Ru^{II} complex is surrounded by H_2O molecules. Higher concentrations of TX-100 result in stabilization of the surfactant micellar aggregate itself and weaker interaction with the luminophore, leading to lower emission intensity and a red shift of the emission peak, due to H_2O solvation of the free complex. The emission lifetimes of complexes **6a** and **6b** do not change significantly upon addition of TX-100, due to nil or weak interaction between luminophore and surfactant, either above or below its *cmc*. This result agrees with the measured fractional exposure to H_2O of these complexes (≥ 0.8, *Table 8*) and is consistent with the similar oxygen-quenching rate constants measured in the presence and in the absence of TX-100 micelles (*Table 9*).

Overall, our results are in agreement with the ample studies carried out by *Demas* and co-workers on the interaction of Ru^{II} photosensitizers with surfactant media [4c]. For instance, they observed an f value of 0.53 for the highly charged complex $[Ru(pbbs)_3]^{4-}$ (**7**) in the presence of SDS, although they did not found any evidence of pre-micellar aggregation. The absence of a hydrophobic ancillary ligand such as pta would account for the difference with **5a**. In the case of their $[Ru(CN)_4(phen)]^{2-}$ (phen = 1,10-phenanthroline), a complex with small anionic head, no binding to SDS was detected. A similar situation occurs with our complexes **6a** and **6b**. When the cationic metal center is well separated from the anionic substituents, electrostatic binding can occur by intercalation of the surfactant head groups between the sulfonated benzene rings. With the bpds complexes and the like, charge separation is small, and interaction with the anionic surfactant is hindered. The anionic $[Ru(CN)_4(phen)]^{2-}$ binds tightly (yet with a high solvent accessibility, $f \approx 0.6$) to the surface of the cationic detergent CTAB due to strong electrostatic attraction [6d]. Microcrystallization of probe·surfactant aggregates was also noticed, in the same way that occurs for complexes **5** and **6** below the surfactant *cmc*. $[Ru(pbbs)_3]^{4-}$ (**7**) also interacts strongly with CTAB ($f \approx 0.3$) [4c], a result paralleled by our pbbs complexes. $[Ru(pbbs)_3]^{4-}$ (**7**) and $[Ru(pbbs)(phen)_2]$ have been shown to promote induced *cmc* of TX-100 [4c][7c] because of the peripheral sulfonate groups, which make the complexes more hydrophilic and decrease the binding strength. It is not a surprise that our pbbs complexes display the highest change of their spectroscopic properties upon binding to TX-100.

Conclusions. – The detailed study on the interaction of a homogeneous family of anionic Ru^{II} complexes with detergents allows identification of the most important factors that control their binding and helps to design future luminescent probes for optical-sensor development. Selectivity to the analyte may be enhanced through a careful design of the metal-complex architecture. Electrostatic factors are of utmost importance to boost or minimize surfactant binding. A high hydrophobicity of the polypyridine chelating ligands ensures strong interactions with detergent molecules. The combination of both factors within a coordinated moiety (such as pbbs (**3a**)) provides the highest sensitivity of the probe to its microenvironment at all surfactant concentrations. A weak binding due to charge repulsion can be partially or largely offset by hydrophobic interactions. In this way, (polypyridine)ruthenium(II) com-

plexes may also be designed to respond non-selectively to a wide variety of detergent molecules.

Experimental Part

General. Solvents: purified H_2O was obtained from a *Milli-Q* system (*Millipore*). All the org. solvents used (MeOH, EtOH, BuOH, AcOH, $CHCl_3$, Et_2O, MeCN, DMF) were of spectroscopic grade. Surfactants and other chemicals: sodium dodecyl sulfate (SDS; *Sigma*), cetyltrimethylammonium bromide (CTAB; *Fluka*), *Triton X-100* (TX100; *Sigma*), β-cyclodextrin (*Aldrich*), NaCl (*Merck*), disodium (1,10-phenanthroline-4,7-diyl)bis-(benzenesulfonate) (pbbs · 2 Na^+; **3a**) (*Fluka*), tris(2,2′-bipyridine-$\kappa N,\kappa N'$)ruthenium (2+) ($[Ru(bpy)_3]^{2+}$; **8**; *Aldrich*). Prep. thin layer chromatography (TLC): silica gel plates, 0.5-mm thick (*Merck 60*). Column chromatography (CC): *Sephadex-LH-20* (*Pharmacia*) stationary phase. M.p.: *Gallenkamp-MFB-595* apparatus; uncorrected. UV/VIS Absorption spectra: *Perkin-Elmer Lambda-3* spectrophotometer; λ_{max} [nm] (ε); at 23 ± 2°. IR Spectra: *Perkin-Elmer 761* or *Pye-Unicam SP3-200* spectrometers; KBr pellets (*Merck*, *Uvasol*); in cm^{-1}. ^1H- and ^{13}C-NMR Spectra: *Varian VXR-300S* spectrometer; in (D_6)DMSO, $CDCl_3$, CD_3OD, or D_2O, > 99% D; at 300 and 75 MHz, resp.; chemical shifts δ in ppm, *J* in Hz. MS: *Varian MAT-711* or *Hewlett-Packard HP-5989A* spectrometers. Elemental analysis: *Perkin-Elmer 2400* CHN analyzer.

Fluorescence, Quantum Yields, and Lifetimes. UV/VIS Emission spectra: *Perkin-Elmer LS-50* spectrofluorometer; at 25 ± 0.5°. Luminescence quantum yields (Φ_{em}): in H_2O, following *Parker* and *Rees*' method [26], with $[Ru(bpy)_3]^{2+}$ (**8**) in H_2O ($\Phi_{em} = 0.042 \pm 0.002$ at 25° under Ar) as reference luminophore [19a][27]; corrected for the different absorption of the reference and sample aq. solns. at the excitation wavelength [28]; at 25.0 ± 0.2° kept with a *Haake D8-GH* circulator; Ar-purged (*N50*, *Praxair*) solns. Luminescence lifetimes (τ): *Edinburgh-Instruments FL-900* time-correlated single photon counting (TC-SPC) apparatus, equipped with a hypobaric N_2 (*N55*, *Praxair*) discharge lamp pulsed at 20 or 40 KHz, and a *Hamamatsu R955* photomultiplier tube (190–850 nm) cooled at −27° with a *Peltier*, connected to an *Ortec 416A* delay generator for the required time windows (0.1–10 μs); at 25.0 ± 0.2° with air-equilibrated, Ar- or O_2-purged (*N40*, *Praxair*) solns. Analysis of the emission profiles without deconvolution of the instrumental response, with the original *Edinburgh-Instruments* software; the decays were fitted, from the peak channel to the baseline of the experimental datapoints, to an exponential function, by means of the least-squares non-linear *Marquardt* algorithm [29]; when necessary, an increasing number of exponentials was added until the fit was statistically acceptable, as judged by the χ^2 test, the appearance of the weighted residuals plot, and the *Durbin-Watson* parameter.

Cyclic Voltammetry and Tensiometry. Cyclic voltammetry: halfwave potentials of the novel $[RuL_2L']^{2-}$ complexes were measured in DMF at 23 ± 2° with an *EG&G-Princeton-Applied-Research-Versastat* system. The three-electrode system consisted of a glassy carbon working electrode (*Metrohm 6.0905.010*), a Pt counter electrode, and a standard calomel electrode (SCE). Tetrabutylammonium hexafluorophosphate (0.1M; *Fluka*) was used as supporting electrolyte. Sample solutions contained $2.0 \cdot 10^{-4}$ M $[RuL_2L']^{2-}$ and were purged with Ar (*C50*; *Carburos Metálicos*). DMF was thoroughly dried over 3-Å molecular sieves (5% *w/v*; *Scharlau*) for at least one week prior to sample preparation. $[Ru(bpy)_3]^{2+}$ (**8**) was used as reference compound ($E^0_{(3+/2+)} = 1.24$ V, $E^0_{(2+/+)} = -1.27$ V [30]). Tensiometry: *Krüss K10-ST* digital tensiometer. Self-aggregation of dissolved $[Ru(pbbs)_2(pta)]^{2-}$ (**5a**) was evaluated by measuring the changes in the absolute surface tension of water following *Wilhelmy*'s method [31]. This procedure allows calculation of the critical micelle concentration (*cmc*) of surfactant molecules by measuring the force between the Pt-plate of the tensiometer and the sample soln. [32]. Such a force is proportional to the surface tension of the surfactant soln. and decreases with the surfactant concentration, until a plateau is reached above the *cmc* of the surfactant. The experiments were performed at 26 ± 1° by addition of 20-μl aliquots of a $2.0 \cdot 10^{-4}$ M aq. soln. of $[Ru(pbbs)_2(pta)]^{2-}$ (**5a**) to the tensiometer vessel filled with 20 ml of purified H_2O. The experiment was performed three times and the results were averaged.

Surfactant Solutions for Luminescence Measurements. Aq. solns. of the $[RuL_2L']^{2-}$ complexes in the presence of surfactants at concentrations of the order of their *cmc*s were prepared, with Ru^{II} complex/detergent ratios providing low micellar occupancy numbers to avoid self-quenching of the luminophore.

The fractional exposure of the micelle-bound luminophores to the aq. phase (*f*) is a parameter that quantitates the part of the metal-complex structure not shielded from the aq. phase by the surfactant molecules. Calculation of this parameter *f* is based on efficient Ru^{II} excited-state quenching by the OH oscillators of the H_2O molecules, according to the method developed by *Demas* and co-workers [6b]: $f = [1/\tau_{H(m)} - 1/\tau_{D(m)}]/[1/\tau_{H(s)} - 1/\tau_{D(s)}]$, where $\tau_{H(m)}$ and $\tau_{D(m)}$ are the luminescence lifetime of the probe in the presence of micelles in H_2O and D_2O, resp., while $\tau_{H(s)}$ and $\tau_{D(s)}$ are the luminescence lifetimes in H_2O and D_2O, resp.

1,10-Phenanthrolin-5-amine (**1**). To a suspension of 5-nitro-1,10-phenanthroline (2.06 g, 9.0 mmol; > 98%; *Sigma*) and 10% Pd/C (0.27 g; *Fluka*) in 90 ml of 95% EtOH, hydrazine hydrate (2.0 ml, 42 mmol; > 99%; *Fluka*) was added dropwise. The mixture was heated for 3 h at 65–70° and then filtered hot through a glass-fiber filter (*Macherey-Nagel MN85/90*) to remove the catalyst. The yellow soln. was concentrated to 25 ml and left at 4° for 24 h. The precipitate was filtered off, washed with cold Et_2O, and dried at 0.007 Torr over P_2O_5 for 24 h: 1.35 g (77%) of **1**. Yellow crystals. M.p. 245–246° ([33]: 259–260°). IR: 3420, 3330, 3230, 3060, 1645, 1620, 1600, 1500, 1440, 840, 750. ^{1}H-NMR ((D$_6$)DMSO): 9.06 (*dd*, *J* = 4.2, 1.7, H–C(2)); 8.69 (*dd*, *J* = 4.2, 1.7, H–C(9)); 8.69 (*dd*, *J* = 8.3, 1.7, H–C(4)); 8.05 (*dd*, *J* = 8.3, 1.7, H–C(7)); 7.74 (*dd*, *J* = 8.3, 4.2, H–C(3)); 7.51 (*dd*, *J* = 8.3, 4.2, H–C(8)); 6.88 (*s*, H–C(6)); 6.13 (*s*, NH_2). ^{13}C-NMR ((D$_6$)DMSO): 177.6 (C(5)); 154.2 (C(2), C(9)); 152.1 (C(10b)); 139.8 (C(6a)); 135.5 (C(4), C(7)); 129.0 (C(10a)); 125.1 (C(3), C(8)); 122.8 (C(4a)); 79.1 (C(6)).

N-*(1,10-Phenanthrolin-5-yl)tetradecanamide* (pta; **2a**). To a soln. of tetradecanoic acid (= myristic acid; 0.52 g, 2.0 mmol; *Aldrich*) in anh. $CHCl_3$ (70 ml) cooled to 0°, Et_3N (0.3 ml, 2.0 mmol; *Merck*) was added dropwise. To this mixture, ethyl carbonochloridate (0.2 ml, 2.0 mmol; *Aldrich*) was added. The cooled mixture was stirred for 30 min, and **1** (0.40 g, 2.0 mmol) was added slowly until complete dissolution. The mixture was left to reach r.t., and then it was refluxed for 2 d. The crude mixture was subsequently washed with dil. HCl soln. at pH 4 (3 × 30 ml), distilled H_2O (2 × 30 ml), sat. Na_2CO_3 soln. (2 × 30 ml), and distilled H_2O (2 × 30 ml). The combined yellowish org. phase was dried ($MgSO_4$) and evaporated, the residue recrystallized from MeOH/H_2O and the product dried at 0.007 Torr over P_2O_5 overnight: **2a** · 2 MeOH (0.37 g, 39%). White microcrystals. M.p. 79–80°. UV/VIS ($CHCl_3$): 270 (19600), 240 (17400). IR: 3400, 3240, 3020, 2940, 2900, 2820, 1640, 1620, 1580, 1530, 1460, 730. ^{1}H-NMR ($CDCl_3$): 9.17 (*d*, *J* = 3.9, H–C(2)); 9.11 (*d*, *J* = 3.9, H–C(9)); 8.28 (*d*, *J* = 8.1, H–C(4)); 8.23 (*s*, NH); 8.18 (*d*, *J* = 8.1, H–C(7)); 7.75 (*s*, H–C(6)); 7.63 (*dd*, *J* = 8.1, 3.9, H–C(3)); 7.61 (*dd*, *J* = 8.1, 3.9, H–C(8)); 2.55 (*t*, *J* = 7.0, 2 H–C(2′)); 1.83 (*quint.*, *J* = 7.0, 2 H–C(3′)); 1.29 (*m*, 20 H); 0.88 (*t*, *J* = 6.6, Me(14′)). ^{13}C-NMR ($CDCl_3$): 172.7 (C=O); 149.5 (C(2), C(9)); 146.1 (C(10b)); 144.1 (C(10a)); 135.6 (C(4)); 130.5 (C(5)); 129.9 (C(7)); 128.0 (C(6a)); 124.1 (C(4a)); 123.2 (C(6)); 122.4 (C(3)); 120.1 (C(8)); 37.2 (C(2′)); 31.8 (C(12′)); 29.5, 29.4, 29.2 (8C); 25.6 (C(3′)); 22.5 (C(13′)); 14.0 (C(14′)). MS: 407 (1.4, $[M+2]^+$); 406 (5.1, $[M+1]^+$); 405 (16.5, *M*); 404 (3.2, $[M-1]^+$); 390 (1.4, $[M-15]^+$); 376 (1.9), 362 (1.9), 348 (1.9), 334 (1.9), 320 (1.4), 306 (1.4), 292 (1.6), 278 (1.2), 264 (1.4) (loss of CH_2 fragments); 250 (5.6, *McLafferty* + 13); 237 (13.0, *McLafferty*); 196 (26.8); 195 (100.0, **1**$^+$). Anal. calc. for $C_{26}H_{35}N_3O \cdot 2\ CH_3OH$: C 72.29, H 8.71, N 8.88; found: C 71.61, H 9.03, N 8.95.

N-*(1,10-Phenanthrolin-5-yl)acetamide* (paa; **2b**). To a soln. of Ac_2O (1.1 ml, 12.0 mmol; *Panreac*) in AcOH (1.8 ml, 30.3 mmol; *Probus*), **1** (0.40 g, 2.0 mmol) was added. The reddish soln. was stirred for 2.5 h at r.t. and then refluxed for 24 h. The cooled crude was poured over distilled H_2O and neutralized with concentrated ammonia solution (*Probus*) to pH 8. The product was recrystallized from EtOH/H_2O, filtered, washed, and dried at 0.007 Torr over P_2O_5 for 24 h: **2b** · H_2O (0.18 g, 35%). White needles. M.p. 231–233°. UV/VIS ($CHCl_3$): 270 (24350), 244 (17200). IR: 3500, 3100, 3000, 1680, 1540, 1510, 1440. ^{1}H-NMR ($CDCl_3$): 8.98 (br. *s*, H–C(2), H–C(9)); 8.73 (*s*, NH); 8.31 (*d*, *J* = 8.0, H–C(4)); 8.02 (*d*, *J* = 8.0, H–C(7)); 7.92 (*s*, H–C(6)); 7.51 (*dd*, *J* = 8.0, 4.0, H–C(3)); 7.41 (*dd*, *J* = 8.0, 4.0, H–C(8)); 2.29 (*s*, Me). ^{13}C-NMR ($CDCl_3$): 169.9 (C=O); 149.8, 149.6 (C(2), C(9)); 146.1 (C(10b)); 144.2 (C(10a)); 135.8 (C(4)); 130.7 (C(5)); 130.3 (C(7)); 128.0 (C(6a)); 124.3 (C(4a)); 123.3 (C(6)); 122.5 (C(3)); 120.4 (C(8)); 24.0 (Me). MS: 238 (5.4, $[M+1]^+$), 237 (31.3, M^+), 195 (100.0, **1**$^+$), 42 (42, CH_2=C=O$^+$). Anal. calc. for $C_{14}H_{11}N_3O \cdot H_2O$: C 64.12, H 5.19, N 16.14; found: C 64.50, H 5.09, N 16.47.

Disodium (2,2′-Bipyridine)-4,4′-disulfonate (bpds · 2 Na$^+$; **3b**). To a suspension of 10% Pd/C (0.51 g; *Fluka*) in anh. MeOH (45 ml), disodium [2,2′-bipyridine]-4,4′-disulfonate 1,1′-dioxide (4.60 g, 11.7 mmol), prepared following the procedure by *Anderson et al.* [12], and anh. ammonium formate (8.00 g, 127 mmol; *Fluka*) were added dropwise. The mixture was heated at 40° for 5.5 h and then filtered through a glass-fiber filter (*Macherey-Nagel MN85/90*) and the filtrate evaporated. The product was redissolved in MeOH/H_2O 4:1, filtered hot through a PTFE membrane (*Millipore, Millex FGS;* 0.2 μm pore size) and precipitated with EtOH. The resulting product was filtered, washed, and dried at 0.007 Torr over P_2O_5 overnight: **3b** · 2 Na$^+$ · 1.5H_2O (1.50 g, 45%). White microcrystals. IR: 3080, 1680, 1580, 1550, 1460, 1240, 1050, 860, 770. ^{1}H-NMR (D_2O): 8.85 (*d*, *J* = 5.1, H–C(6), H–C(6′)); 8.44 (*d*, *J* = 1.3, H–C(3), H–C(3′)); 7.88 (*dd*, *J* = 5.1, 1.3, H–C(5), H–C(5′)). ^{13}C-NMR (D_2O): 158.5 (C(2), C(2′)); 155.1 (C(6), C(6′)); 153.5 (C(4), C(4′)); 123.5 (C(5), C(5′)); 121.1 (C(3), C(3′)). Anal. calc. for $C_{10}H_6N_2Na_2O_6S_2 \cdot 1.5H_2O$: C 30.87, H 2.27, N 7.19; found: C 31.01, H 2.34, N 7.24.

Tetrasodium Dichlorobis[(1,10-phenanthroline-4,7-diyl-κN,κN′)bis(benzenesulfonato)(2−)]ruthenate(4−) (**4a**) *and Tetrasodium Bis[(2,2′-bipyridine)-4,4′-disulfonato(2−)-κN,κN′]dichlororuthenate(4−)* (**4b**): *General Procedure.* To a mixture of pbbs · 2 Na$^+$ (**3a** · 2 Na$^+$; *Fluka*) or bpds · 2 Na$^+$ (**3b** · 2 Na$^+$) (2.05 mmol) and $RuCl_3$ ·

$3H_2O$ (1 mmol; *Aldrich*) in DMF (6 ml; 99,5%; *Panreac*), LiCl (6.0 mmol; *Panreac*) was added. The soln. was refluxed for 5 h (pbbs complex) or 24 h (bpds complex) under Ar. The mixture at r.t. was poured in a beaker and kept inside a closed container under acetone atmosphere for 3 d. The respective products obtained were filtered off, washed with cold acetone, and dried at 0.007 Torr for 24 h over P_2O_5: **4a** · 4 Na^+ · $8H_2O$ · 4 LiCl (1.37 g, 88%) or **4b** · 4 Na^+ · $4H_2O$ · 25 LiCl (0.85 g, 42%) as violet microcrystals. UV/VIS Data of **4a** · 4 Na^+ · $4H_2O$ · 25 LiCl (H_2O): 465 (11600), 227 (61200). UV/VIS (DMF): 567 (8800), 476 (10300), 282 (70400). IR: 3060, 1640, 1190, 1040. Anal. calc. for $C_{48}H_{28}Cl_2N_4Na_4O_{12}RuS_4 \cdot 8H_2O \cdot 4$ LiCl: C 36.76, H 2.87, N 3.92; found: C 36.99, H 2.85, N 3.59. Data of **4b** · 4 Na^+ · $4H_2O$ · 25 LiCl (H_2O): 516 (2740), 366 (8750), 301 (14600). (DMF): 564 (7700), 388 (9600), 303 (47100), 250 (24100). Anal. calc. for $C_{20}H_{12}Cl_2N_4Na_4O_{12}RuS_4 \cdot 4H_2O \cdot 25$ LiCl: C 11.51, H 0.87, N 3.22; found: C 11.87, H 1.00, N 2.88.

Heteroleptic Complexes **5** *and* **6** *($Na_2[RuL_2L']$): General Procedure.* A mixture of **4a** or **4b** (1 mmol) and **2a** or **2b** (2.0 mmol) in MeOH (40 ml) under Ar was refluxed for 24 h. Different purification procedures were applied to the mixture (see below).

Disodium Bis[(1,10-phenanthroline-4,7-diyl-κN,κN′)bis(benzenesulfonato)(2−)][N-(1,10-phenanthrolin-5-yl-κN,κN′)tetradecanamide]ruthenate(2−) (**5a** · 2 Na^+): The complex was precipitated from the mixture with acetone/H_2O 9:1, filtered off, washed with Et_2O, and purified by prep. TLC (BuOH/AcOH/H_2O 7:3:4). The fraction containing the pure complex was desorbed with MeOH to yield **5a** · 2 Na^+ · 11 H_2SiO_3 (0.45 g, 19%). Orange microcrystals. UV/VIS (H_2O): 460 (36600), 427 (35650), 274 (175800). UV/VIS (MeOH): 457 (30000), 430 (28550), 278 (110000). IR: 2940, 2850, 1640, 1570, 1420, 1190, 1050, 810. ^{1}H-NMR (CD_3OD): 8.80 (*d*, *J* = 7.5, 1 H); 8.63 (*d*, *J* = 9.0, 1 H); 8.55 (br. *s*, 1 H); 8.44–8.34 (*m*, 3 H); 8.30–8.20 (*m*, 6 H); 8.04 (br. *s*, 2 H); 8.02–7.90 (*m*, 6 H), 7.76–7.60 (*m*, 16 H); 2.64 (*t*, *J* = 6.8, 2 H−C(2′)); 1.80 (*t*, *J* = 6.8, 2 H−C(3′)); 1.47 (*m*, 2 H−C(4′)); 1.26 (br. *s*, 18 H); 0.86 (*t*, *J* = 6.0, Me). Anal. calc. for $C_{74}H_{63}N_7Na_2O_{13}RuS_4 \cdot 11$ H_2SiO_3: C 36.81, H 3.23, N 4.21; found: C 37.15, H 3.48, N 4.10.

Disodium Bis[(1,10-phenanthroline-4,7-diyl-κN,κN′)bis(benzenesulfonato)(2−)][N-(1,10-phenanthrolin-5-yl-κN,κN′)acetamide]ruthenate(2−) (**5b** · 2 Na^+). The complex was precipitated from the mixture with acetone/Et_2O 9:1. The precipitate was filtered off, washed with Et_2O, and then precipitated again from MeOH/Et_2O. The product was filtered, washed with $CHCl_3$, and dried at 0.007 Torr over P_2O_5 overnight: **5b** · 2 Na^+ · $8H_2O$ (0.75 g, 50%). Orange microcrystals. UV/VIS (H_2O): 459 (22700), 435 (22550), 275 (102000), 215 (98600). IR: 1630, 1550, 1420, 1180, 1050, 840. ^{1}H-NMR (CD_3OD): 8.83 (*d*, *J* = 8.3, 1 H); 8.64 (*d*, *J* = 8.3, 1 H); 8.56 (br. *s*, 1 H); 8.46–8.34 (*m*, 3 H); 8.32–8.23 (*m*, 6 H); 8.12–7.96 (*m*, 8 H); 7.88–7.58 (*m*, 16 H); 2.36 (br. *s*, Me). Anal. calc. for $C_{62}H_{39}N_7Na_2O_{13}RuS_4 \cdot 8H_2O$: C 49.30, H 3.46, N 6.02; found: C 49.33, H 3.64, N 6.29.

Disodium Bis[(2,2′-bipyridine)-4,4′-disulfonato(2−)-κN,κN′][N-(1,10-phenanthrolin-5-yl-κN,κN′)tetradecanamide]ruthenate(2−) (**6a** · 2 Na^+). The mixture was filtered and the solid product washed with MeOH, dried at reduced pressure, and recrystallized from MeOH. Further recovery of the product from the mixture was achieved by CC (MeOH) followed by reprecipitation with MeOH/MeCN. The product was filtered off, washed with cold MeCN, and dried at 0.007 Torr over P_2O_5 for 24 h: **6a** · $2Na^+$ · $9H_2O$ (0.55 g, 41%). Orange microcrystals. UV/VIS (H_2O): 466 (17500), 434 (15600), 296 (67000), 266 (42300), 218 (72000). IR: 2900, 2840, 1620, 1530, 1420, 1220, 1060, 760. ^{1}H-NMR (CD_3OD): 9.00 (*d*, *J* = 1.5, 2 H−C(3) of bpds); 8.95 (*s*, *J* = 1.5, 2 H−C(3) of bpds); 8.77 (*dd*, *J* = 8.4, 1.1, H−C(4)); 8.63 (*dd*, *J* = 8.4, 1.1, H−C(7)); 8.52 (*s*, H−C(6)); 8.20 (*dd*, *J* = 5.4, 1.1, H−C(2)); 8.13 (*d*, *J* = 5.6, 2 H−C(6) of bpds); 8.11 (*dd*, *J* = 5.4, 1.1, H−C(9)); 7.98 (*s*, 0.5 H, CON*H*); 7.96 (*s*, 0.5 H, CON*H*); 7.86 (*dd*, *J* = 8.4, 5.4, H−C(3)); 7.84 (*dd*, *J* = 5.6, 1.5, 2 H−C(5) of bpds); 7.80 (*dd*, *J* = 8.4, 5.4, H−C(8)); 7.73 (*d*, *J* = 5.6, 2 H−C(6) of bpds); 7.58 (*dd*, *J* = 5.6, 1.5, 2 H−C(5) of bpds); 2.64 (*t*, *J* = 7.0, 2 H−C(2′)); 1.82 (*quint.*, *J* = 7.0, 2 H−C(3′)); 1.44 (*m*, 20 H); 0.89 (*t*, *J* = 6.3, Me). Anal. calc. for $C_{46}H_{47}N_7Na_2O_{13}RuS_4 \cdot 9H_2O$: C 41.01, H 3.98, N 7.36; found: C 41.13, H 3.88, N 7.30.

Disodium Bis[(2,2′-bipyridine)-4,4′-disulfonato(2−)-κN,κN′][N-(1,10-phenanthrolin-5-yl-κN,κN′)acetamide]ruthenate(2−) (**6b** · 2 Na^+). The mixture was dissolved in MeOH/H_2O 10:1 and filtered hot to remove unreacted ligand **2b**. The filtrate was evaporated, and the residue reprecipitated from EtOH/H_2O. The product was dried at 0.007 Torr over P_2O_5 overnight: **6b** · 2 Na^+ · $9H_2O$ (0.93 g, 79%). Orange microcrystals. UV/VIS (H_2O): 466 (16800), 446 (16100), 296 (64500), 264 (44800), 218 (71700). IR: 1620, 1540, 1400, 1220, 1040, 760. ^{1}H-NMR (CD_3OD): 8.99 (*d*, *J* = 1.5, 2 H−C(3) of bpds); 8.95 (*d*, *J* = 1.5, 2 H−C(3) of bpds); 8.82 (*dd*, *J* = 8.4, 1.2, H−C(4)); 8.63 (*dd*, *J* = 8.4, 1.2, H−C(7)); 8.54 (*s*, H−C(6)); 8.19 (*dd*, *J* = 5.1, 1.2, H−C(2)); 8.11 (*d*, *J* = 5.9, 2 H−C(6) of bpds); 8.10 (*dd*, *J* = 5.1, 1.2, H−C(9)); 7.97 (*s*, 0.5 H, CONH); 7.95 (*s*, 0.5 H, CONH); 7.86 (*dd*, *J* = 8.4, 5.1, H−C(3)); 7.83 (*dd*, *J* = 5.9, 1.5, 2 H−C(5) of bpds); 7.79 (*dd*, *J* = 8.4, 5.1, H−C(8)); 7.72 (*d*, *J* = 5.9, 2 H−C(6) of bpds); 7.57 (*dd*, *J* = 5.9, 1.5, 2 H−C(5) of bpds); 2.36 (*s*, Me). Anal. calc. for $C_{34}H_{23}N_7Na_2O_{13}RuS_4 \cdot 9H_2O$: C 34.60, H 3.01, N 8.25; found: C 34.75, H 3.12, N 8.34.

Tetrasodium Tris[(1,10-phenanthroline-4,7-diyl-κN,κN′)bis(benzenesulfonato)(2−)]ruthenate(4−) (**7**·4 Na^+). To a soln. of $RuCl_3 \cdot 3H_2O$ (0.02 g, 0.10 mmol; *Aldrich*) in EtOH/H_2O (9 ml), **3a**·2 Na^+ (0.2 g, 0.35 mmol; *Fluka*) was added under Ar, and the mixture was heated under reflux for 5 h. At r.t., the mixture was filtered, the filtrate evaporated, and the residue reprecipitated as a colloid from EtOH/H_2O. The slurry was centrifuged at 4000 rpm, the orange solid washed thoroughly with EtOH, and the product dried at 0.007 Torr over P_2O_5 overnight: **7**·4 $Na^+ \cdot 12H_2O$ (0.12 g, 64%). UV/VIS (H_2O): 462 (29300), 438 (29100), 278 (121300), 216 (116400). UV-VIS (MeOH): 463 (32400), 438 (32100), 279 (137900), 219 (126600). IR: 1420, 1190, 1050. Anal. calc. for $C_{72}H_{42}N_6Na_4O_{18}RuS_6 \cdot 12H_2O$: C 45.78, H 3.55, N 4.41; found: C 45.98, H 3.54, N 4.47.

We are grateful to the Spanish Government agency *CICYT* (*R + D National Plan*) for financial support through projects *AMB98-1043-C02-01* and *PPQ2000-0778-C02-01*, as well as the *Madrid Community Government* (*CAM*, project no. 07/0082/2000). *D. G.-F.* thanks the Complutense University for a pre-doctoral grant. The authors thank *Ana M. Castro* and *C. Knapp* (UCM) for helpful assistance in the synthesis of the Ru^{II} complexes.

REFERENCES

[1] a) N. J. Turro, M. Grätzel, A. M. Braun, *Angew. Chem., Int. Ed.* **1980**, *19*, 675; b) K. Kalyanasundaram, 'Photochemistry in Microheterogeneous Systems', Academic Press, Orlando, 1987; c) 'Photochemistry in Organized and Constrained Media', Ed. V. Ramamurthy, VCH Publishers, New York, 1991; d) R. von Wandruszka, *Crit. Rev. Anal. Chem*. **1992**, *23*, 187; e) 'Topics in Fluorescence Spectroscopy', Ed. J. R. Lakowicz, Plenum Press, New York, 1994, Vol. 4.

[2] a) J. N. Demas, B. A. DeGraff, *Anal. Chem*. **1991**, *63*, 829A; b) A. Juris, V. Balzani, F. Barigelletti, S. Campagna, P. Belser, A. Von Zelewsky, *Coord. Chem. Rev*. **1988**, *84*, 85.

[3] a) J. N. Demas, B. A. DeGraff, 'Design and Applications of Highly Luminescent Transition Metal Complexes', in 'Topics in Fluorescence Spectroscopy', Ed. J. R. Lakowicz, Plenum Press, New York, 1994, Vol. 4, p. 71; b) G. Orellana, D. García-Fresnadillo, M. D. Marazuela, M. C. Moreno-Bondi, J. Delgado, J. M. Sicilia, 'Fibre-Optic Chemical Sensors: from Molecular Engineering to Environmental Analytical Chemistry In the Field', in 'Monitoring of Water Quality: The Contribution of Advanced Technologies', Ed. F. Colin, P. Quevauviller, Elsevier, Amsterdam, 1998, p. 103.

[4] a) P. Serguievski, W. E. Ford, M. A. J. Rodgers, *Langmuir* **1996**, *12*, 348; b) G. Bünau, T. Wolff, *Adv. Photochem.* **1988**, *14*, 273; c) S. W. Snyder, S. L. Buell, J. N. Demas, B. A. DeGraff, *J. Phys. Chem.* **1989**, *93*, 5265; d) A. Kirsch-De Mesmaeker, J. P. Lecomte, J. M. Kelly, *Topics Curr. Chem.* **1996**, *177*, 25; e) C. Moucheron, A. Kirsch-De Mesmaeker, J. M. Kelly, *Struct. Bonding* **1998**, *92*, 163; f) E. Gicquel, N. Paillous, P. Vicendo, *Photochem. Photobiol.* **2000**, *72*, 583; g) G. L. Duveneck, C. V. Kumar, N. J. Turro, J. K. Barton, *J. Phys. Chem.* **1988**, *92*, 2028; h) R. Ramaraj, P. Natarajan, *J. Polym. Sci.* **1991**, *29*, 1339; i) H. D. Gafney, *Coord. Chem. Rev.* **1990**, *104*, 113; j) P. V. Kamat, W. E. Ford, *Photochem. Photobiol.* **1992**, *55*, 159; k) K. Maruszewski, D. P. Strommen, K. Handrich, J. R. Kincaid, *Inorg. Chem.* **1991**, *30*, 4579; l) M. C. Moreno-Bondi, G. Orellana, N. J. Turro, *Macromolecules* **1990**, *23*, 910.

[5] a) 'Molecular Dynamics in Restricted Geometries', Ed. J. Klafter, J. M. Drake, John Wiley and Sons, New York, 1989; b) M. H. Gehlen, F. DeSchryver, *Chem. Rev*. **1993**, *93*, 199; c) P. Lianos, *Heterogen. Chem. Rev.* **1996**, *3*, 53.

[6] a) W. J. Dressick, B. L. Hauenstein, J. N. Demas, B. A. DeGraff, *Inorg. Chem*. **1984**, *23*, 1107; b) B. L. Hauenstein, W. J. Dressick, S. L. Buell, J. N. Demas, B. A. DeGraff, *J. Am. Chem. Soc*. **1983**, *105*, 4251; c) W. J. Dressick, B. L. Hauenstein, T. B. Gilbert, J. N. Demas, B. A. DeGraff, *J. Phys. Chem*. **1984**, *83*, 3337; d) S. W. Snyder, J. N. Demas, B. A. DeGraff, *Chem. Phys. Lett.* **1988**, *145*, 434.

[7] a) W. J. Dressick, K. W. Raney, J. N. Demas, B. A. DeGraff, *Inorg. Chem*. **1984**, *83*, 875; b) B. L. Hauenstein, W. J. Dressick, T. B. Gilbert, J. N. Demas, B. A. DeGraff, *J. Phys. Chem*. **1984**, *88*, 1902; c) B. L. K. Krisnagopal Mandal, B. L. Hauenstein, J. N. Demas, B. A. DeGraff, *J. Phys. Chem*. **1983**, *87*, 328.

[8] a) U. Lachish, M. Ottolenghi, J. Rabani, *J. Am. Chem. Soc*. **1977**, *99*, 8062; b) J. H. Baxendale, M. A. J. Rodgers, *J. Phys. Chem*. **1982**, *86*, 4906.

[9] a) J. I. Cline, W. J. Dressick, J. N. Demas, B. A. DeGraff, *J. Phys. Chem*. **1985**, *89*, 94; b) K. Gooding, K. Johnson, L. Lefkowitz, B. M. Williams, *J. Chem. Educ*. **1994**, *71*, A8.

[10] R. Nasielski-Hinkens, M. Benedek-Vamos, D. Maetens, *J. Heterocycl. Chem*. **1980**, *17*, 873.

[11] D. H. R. Barton, F. Comer, D. G. T. Creig, P. G. Sammes, M. C. Cooper, G. Hewitt, W. G. E. Underwood, *J. Chem. Soc. C* **1971**, 3540.

[12] S. Anderson, E. C. Constable, K. R. Seddon, J. E. Turp, J. E. Baggott, M. J. Pilling, *J. Chem. Soc., Dalton Trans.* **1985**, 2247.
[13] R. Balicki, *Synthesis* **1989**, 645.
[14] B. P. Sullivan, D. J. Salman, T. J. Meyer, *Inorg. Chem*. **1978**, *17*, 3334.
[15] R. A. Krause, *Struct. Bonding* **1987**, *67*, 1.
[16] E. A. Seddon, K. R. Seddon, 'The Chemistry of Ruthenium', in 'Topics in Inorganic and General Chemistry', Ed. R. J. H. Clark, Elsevier, Amsterdam, 1984, Vol. 19, p. 1173.
[17] M. J. Cook, A. P. Lewis, G. S. G. McAuliffe, V. Skarda, A. J. Thomson, J. L. Glasper, D. J. Robbins, *J. Chem. Soc., Perkin Trans. 2* **1984**, 1303; P. C. Alford, M. J. Cook, A. P. Lewis, G. S. G. McAuliffe, V. Skarda, A. J. Thompson, J. L. Glasper, D. J. Robbins, *J. Chem. Soc., Perkin Trans. 2* **1985**, 705.
[18] D. García-Fresnadillo, Y. Georgiadou, G. Orellana, A. M. Braun, E. Oliveros, *Helv. Chim. Acta* **1996**, *79*, 1222.
[19] a) J. Van Houten, R. J. Watts, *J. Am. Chem. Soc*. **1976**, *98*, 4853; b) A. Pfeil, *J. Am. Chem. Soc*. **1971**, *93*, 5395.
[20] S. L. Murov, I. Carmichael, G. L. Hug, 'Handbook of Photochemistry', 2nd edn., Marcel Dekker, New York, 1993.
[21] E. R. Carraway, J. N. Demas, B. A. DeGraff, *Anal. Chem*. **1991**, *63*, 332; M. P. Xavier, D. García-Fresnadillo, M. C. Moreno-Bondi, G. Orellana, *Anal. Chem.* **1998**, *70*, 5184; D. García Fresnadillo, M. D. Marazuela, M. C. Moreno Bondi, G. Orellana, *Langmuir* **1999**, *15*, 6451.
[22] 'Organic Electrochemistry: an Introduction and a Guide', Ed. M. M. Baizer, H. Lund, Marcel Dekker, New York, 1983.
[23] C. T. Lin, W. Bötcher, M. Chou, C. Creutz, N. Sutin, *J. Am. Chem. Soc.* **1976**, *98*, 6536.
[24] G. Orellana, M. L. Quiroga, A. M. Braun, *Helv. Chim. Acta* **1987**, *70*, 2073.
[25] P. Mukerjee, K. Mysels, *J. Am. Chem. Soc.* **1955**, *77*, 2437.
[26] K. D. Mielenz, 'Measurement of Photoluminescence', in 'Optical Radiation Measurements', Ed. F. Grum, C. J. Bartleson, Academic Press, New York, 1982, Vol. 3.
[27] J. V. Caspar, T. J. Meyer, *J. Am. Chem. Soc.* **1983**, *105*, 5583.
[28] D. F. Eaton, *Pure Appl. Chem*. **1988**, *60*, 1107.
[29] S. W. Snyder, J. N. Demas, B. A. DeGraff, *Anal. Chem.* **1989**, *61*, 2704; D. V. O'Connor, D. Phillips, 'Time-Correlated Single Photon Counting', Academic Press, London, 1984.
[30] C. M. Elliott, E. J. Hersenhart, *J. Am. Chem. Soc*. **1982**, *104*, 7519.
[31] 'GIT Fachzeitschrift für das Laboratorium', 'Measurement of Interfacial Tension and Surface Tension – General Review for Practical Man', GIT Verlag GmbH, Darmstadt, 1980, Vol. 24, p. 642–648 and 734–742; J. Höpken, M. Möller, *Macromolecules* **1992**, *25*, 1461.
[32] P. Mukerjee, K. J. Mysels, 'Critical Micelle Concentrations of Aqueous Surfactant Systems', NSRDS-NBS *36*, U.S. Dept. of Commerce, Washington D.C., 1971.
[33] E. Koft, C. H. Case, *J. Org. Chem*. **1962**, *27*, 865.
[34] C. de Dios, Ph.D. Thesis, Universidad Complutense de Madrid, 1994.
[35] M. Maestri, M. Grätzel, *Ber. Bunsenges. Phys. Chem*. **1977**, *81*, 504.
[36] Y. Kawanishi, N. Kitamura, Y. Kim, S. Tazuki, *Sci. Pap. Inst. Phys. Chem. Res.* **1984**, *78*, 212.

Received May 31, 2001